CELL CYCLE
2016, VOL. 15, NO. 13, 1733–1741
http://dx.doi.org/10.1080/15384101.2016.1183853

Taylor & Francis
Taylor & Francis Group

REPORT

AS160 controls eukaryotic cell cycle and proliferation by regulating the CDK inhibitor p21

Pianchou Gongpan[a,b], Yanting Lu[a,b], Fang Wang[a,b], Yuhui Xu[a,b], and Wenyong Xiong[a]

[a]State Key Laboratory of Phytochemistry and Plant Resources in West China, Kunming Institute of Botany, Chinese Academy of Sciences, Kunming, Yunnan, P.R. China; [b]Graduate University of Chinese Academy of Sciences, Beijing, P.R. China

ABSTRACT

AS160 (TBC1D4) has been implicated in multiple biological processes. However, the role and the mechanism of action of AS160 in the regulation of cell proliferation remain unclear. In this study, we demonstrated that AS160 knockdown led to blunted cell proliferation in multiple cell types, including fibroblasts and cancer cells. The results of cell cycle analysis showed that these cells were arrested in the G1 phase. Intriguingly, this inhibition of cell proliferation and the cell cycle arrest caused by AS160 depletion were glucose independent. Moreover, AS160 silencing led to a marked upregulation of the expression of the cyclin-dependent kinase inhibitor p21. Furthermore, whereas AS160 overexpression resulted in p21 downregulation and rescued the arrested cell cycle in AS160-depeleted cells, p21 silencing rescued the inhibited cell cycle and proliferation in the cells. Thus, our results demonstrated that AS160 regulates glucose-independent eukaryotic cell proliferation through p21-dependent control of the cell cycle, and thereby revealed a molecular mechanism of AS160 modulation of cell cycle and proliferation that is of general physiological significance.

ARTICLE HISTORY
Received 16 March 2016
Revised 20 April 2016
Accepted 22 April 2016

KEYWORDS
AS160/TBC1D4; cell cycle; cell proliferation; G1/S; p21

Introduction

AS160 (TBC1D4), a GTPase-activating protein (GAP) that functions downstream from Akt,[1] inhibits the activity of the small GTPases that control intracellular trafficking of vesicles, including the vesicles that traffic GLUT4, insulin, AQP2, Na^+/K^+-ATPase, and Na^+ channels.[2-6] In adipose tissues and skeletal muscles in particular, AS160 has been extensively studied in the control of GLUT4 transport in response to insulin: AS160 modulates GLUT4 transport through a PI3-kinase-dependent mechanism by directly regulating the activities of Rab10, Rab13, and/or Rab8,[7-10] and its role in this process has been partially supported by experiments conducted *in vivo*.[11-15]

Emerging evidence indicates that AS160 also functions in other biological processes, including the regulation of R-wave amplitude in the heart and lipid droplet fusion and growth.[16,17] Recently, one study reported that AS160 might play a central role in β-cell function and survival: Primary cultures of β-cells and MIN6B1 cells expressing reduced levels of AS160 showed increased apoptosis and a loss of glucose-induced proliferation, as revealed through the measurement of 5-bromo-2′-deoxyuridine incorporation.[6] TBC1D1, a paralog of TBC1D4, has also been shown to affect rat β-cell function and survival.[18] Moreover, AS160 phosphorylation at the key residue T642 (p-AS160) was markedly higher in breast cancer tissue than in normal adjacent tissues; here, p-AS160 was positively correlated with tumor size and the cell-proliferation marker Ki-67.[19] These results indicated a potential role of AS160 in cell proliferation. However, the exact role played by AS160 in cell proliferation is unclear, and the molecular mechanism by which AS160 regulates cell proliferation remains unknown.

In this study, we comprehensively demonstrated that AS160 silencing blunted cell proliferation at the rapid-growth phase by arresting fibroblasts and various cancer cells in the G1 phase, and that AS160 produced its effect on cell cycle by regulating the cyclin-dependent kinase (CDK) inhibitor p21 in multiple cell types. Our findings reveal a clear function and mechanism of action of AS160 in the modulation of eukaryotic cell proliferation, which might be of broad physiological significance.

Results

AS160 knockdown suppresses cell proliferation and induces cell cycle arrest in the G1 phase in multiple cell types

To determine the role of AS160 in cell proliferation, we first knocked down AS160 protein expression in mouse 3T3-L1 fibroblasts by using shRNA against the most reported AS160 target sequence,[9] and then monitored the cell numbers for 5 d.[20] The AS160-specific shRNA but not control shRNA efficiently and stably reduced AS160 expression in 3T3-L1 fibroblasts (>90% depletion; Fig. 1A); notably, the proliferation of these cells was inhibited by approximately 50% in the rapid-

CONTACT Wenyong Xiong Ph.D xiong.wenyong@mail.kib.ac.cn Kunming Institute of Botany, Chinese Academy of Sciences 132 Lanhei Road, Kunming, Yunnan, China.
Supplemental data for this article can be accessed on the publisher's website.

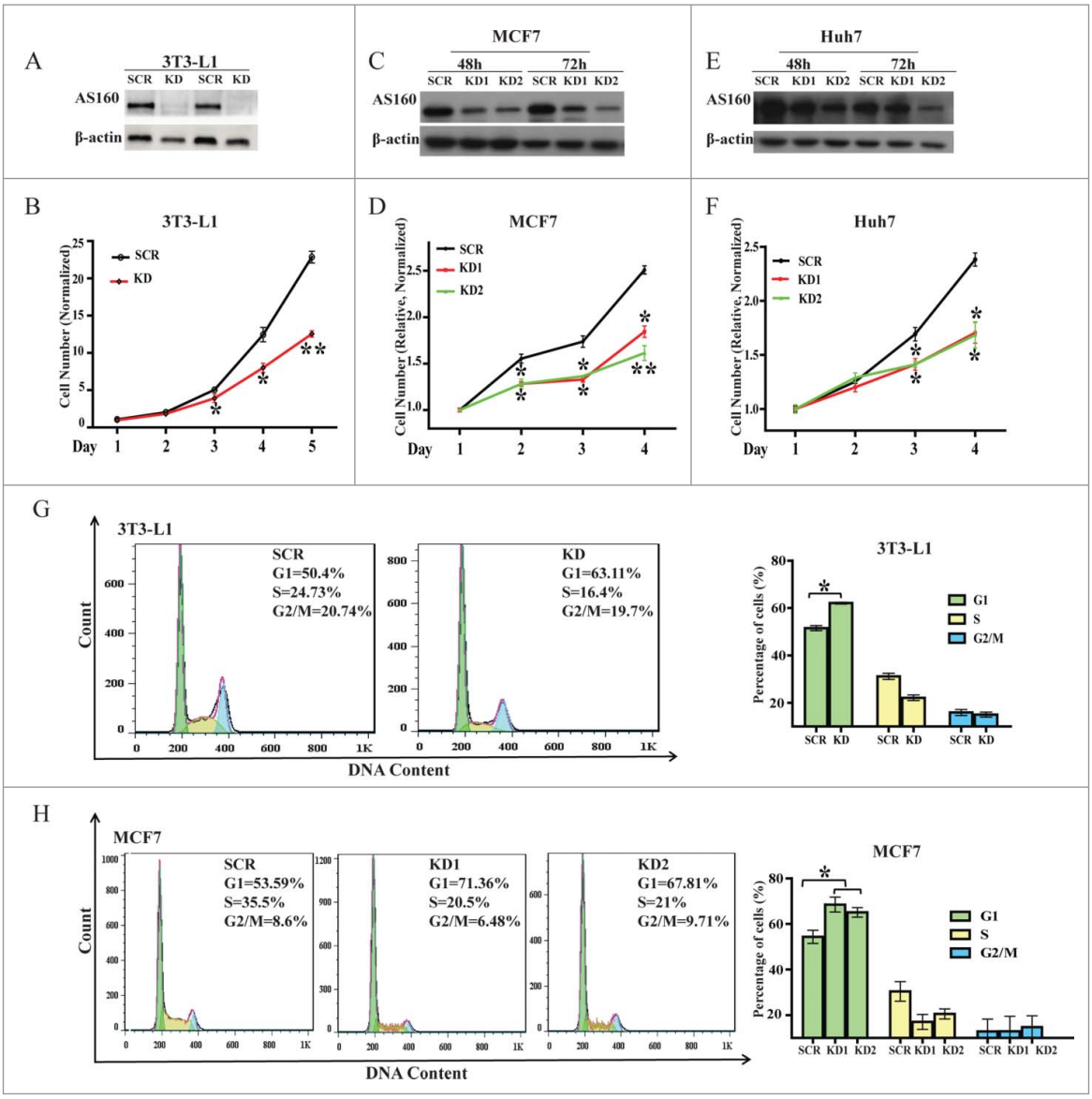

Figure 1. AS160 silencing suppresses cell proliferation and induces cell cycle arrest in the G1 phase in multiple cell types. (A) Levels of the indicated protein in 3T3-L1 fibroblasts infected with a scrambled (SCR) or AS160-specific shRNA (KD) were determined by performing protein gel blotting with duplicate sample loading; β-actin served as a loading control. (B) Proliferation of cells from (A) was determined by counting cells and normalizing the numbers relative to the initial cell numbers. Data represent mean ± s.e.m. ($n = 3$ represents 3 replicated experiments, same below); here and below, $^{*}p < 0.05$ and $^{**}p < 0.01$ compared to SCR, 2-tailed t test. (C) Western blots of MCF7 cells transfected with 2 AS160 siRNAs (KD1 and KD2) or scrambled siRNA (SCR), at 48 and 72 h post-transfection. (D) Proliferation levels of MCF7 cells from (C) were determined using the MTS assay and normalized relative to the respective initial OD values. Data represent mean ± s.e.m. ($n = 3$). (E) Western blots of Huh7 cells transfected with 2 AS160 siRNAs (KD1 and KD2) or scrambled siRNA (SCR), at 48 and 72 h post-transfection. (F) Proliferation levels of Huh7 cells from (E) were determined using the MTS assay and normalized relative to the respective initial OD values. Data represent mean ± s.e.m. ($n = 3$). (G) Cell cycle analysis of SCR and K_D 3T3-L1 fibroblasts. Results represent percentages of cells in G1, S, and G2/M phases for the representative experiment (left) and mean ± s.e.m. (right, $n = 3$); here and below, $^{*}p < 0.05$ compared to SCR, t test. (H) Cell cycle analysis of MCF7 cells transfected with 2 AS160 siRNAs (KD1 and KD2) or scrambled siRNA (SCR).

growth phase (starting from the third day; Fig. 1B). Next, we tested whether this role of AS160 in cell proliferation applies broadly to other cell types. Given that cancer cells grow faster than normal cells, we evaluated cell proliferation in 2 human cancer cell lines, MCF7 and Huh7. As per our expectation, both of the AS160-specific siRNAs that we tested (see Methods) silenced AS160 expression by 50%–70% in these cells (Figs 1C, E), and this was sufficient for markedly inhibiting the proliferation of these cells (Figs 1D, F).

Apoptosis occurs normally during development and aging and serves as a homeostatic mechanism for maintaining cell populations in tissues. To determine whether the regulatory effect of AS160 on cell proliferation was specific, we examined how AS160 depletion affected apoptosis. As expected, apoptosis analysis performed using Annexin-V/propidium iodide (PI) staining and flow cytometry revealed that shRNA-mediated AS160 depletion did not affect apoptosis in 3T3-L1 fibroblasts (Fig. S1).

A critical mechanism for controlling the proliferation of cells is the cell cycle. Thus, to further characterize the effect of AS160 in the regulation of cell proliferation, we next tested whether AS160 knockdown affects the cell cycle in various cell types. The results of flow cytometric analysis revealed that in 3T3-L1 fibroblasts, the AS160-specific shRNA induced the

arrest of 63.11% of the cells in the G1 phase, whereas the scrambled shRNA induced the G1 arrest of 50.40% of the cells (Fig. 1G). Moreover, this effect was not limited to 3T3-L1 fibroblasts: AS160 silencing in MCF7 cells by using the 2 specific siRNAs caused the G1 arrest of 71.36% and 67.81% of the cells as compared to 53.59% with the scrambled siRNA (Fig. 1H).

Altering glucose or lactate does not rescue increased G1 arrest or blunted cell proliferation induced by AS160 depletion

AS160 has been mostly reported to function as a GAP for the small GTPases that control GLUT4 trafficking to the plasma membrane; this indicates that AS160 is related to glucose uptake, metabolism, and homeostasis. Therefore, we investigated whether the effect of AS160 depletion on the proliferation of 3T3-L1 fibroblasts is directly related to the amount of glucose and metabolic lactate in these cells.

Because 3T3-L1 cells have been extensively used for studying adipogenesis, we first evaluated whether AS160-depleted 3T3-L1 fibroblasts can undergo normal differentiation. Here, AS160 knockdown did not affect the differentiation of 3T3-L1 fibroblasts into adipocytes, as revealed by oil red staining and quantification (Fig. 2A). Moreover, we introduced an HA-GLUT4-GFP construct into the adipocytes and then imaged GLUT4 distribution and quantified its surface-to-total ratio. As expected, AS160 depletion also induced a 2-fold increase in GLUT4 distribution to the plasma membrane (Fig. 2B) and increased glucose uptake under basal conditions in differentiated adipocytes (Fig. 2C), which indicated that these 3T3-L1 fibroblasts were capable of normal and functional differentiation.

Next, we measured glucose uptake in 3T3-L1 fibroblasts. Our results demonstrated that AS160-depleted 3T3-L1 fibroblasts maintained an increased glucose-uptake level (relative to control) during the entire growth period (Fig. 2D), which led us to investigate whether artificially altering glucose levels in the culture medium can rescue the AS160-depletion-dependent inhibited cell proliferation and/or arrested cell cycle. In addition to using the normal conditions, we added 10 or 5 mM glucose to scrambled-siRNA-treated cells (scramble cells) and AS160-depleted cells, respectively; the use of this approach resulted in an equal amount of glucose being taken up into the scramble and AS160-depleted cells (Fig. 2E). Under these conditions, the scramble cells exhibiting increased glucose uptake still maintained a lower percentage (~31%) of cells in G1, whereas the AS160-depleted cells exhibiting reduced glucose uptake maintained a higher percentage (~49%) of cells in G1 (Fig. 2E, F). Thus, although we ensured that the overall amount of glucose uptake into these cells was same by altering the glucose level in the culture medium, the percentage of scramble and AS160-depleted cells in the G1 and S phases differed significantly (Fig. 2E, F, black and blue bars).

In addition to the increased glucose uptake in AS160-depleted 3T3-L1 fibroblasts, we expected to observe an increase in the lactate level in the culture medium; accordingly, measurement of lactate levels revealed that lactate was maintained at higher levels relative to control in the culture medium of AS160-depleted cells during a 4-d growth period (Fig. 2G). Thus, to determine whether or not the effect on cell proliferation in AS160-depleted cells is related to this increased lactate level, we added an extra 0.6 mM lactate in the medium used for culturing the scramble cells; this ensured that the lactate levels were equal in the culture medium of both scramble cells and AS160-depleted cells (Fig. 2H). Our results showed that the scramble cells exposed to additional lactate grew at the same rate as the regular scramble cells even when we examined a longer (7-d) growth period (Fig. 2I), which revealed that the blunted cell proliferation in the AS160-depleted cells was not related to the metabolic end-product lactate. Collectively, these data indicated that AS160-regulated cell proliferation is independent of glucose-related mechanism(s).

AS160 knockdown upregulates the expression of the CDK inhibitor p21 in multiple cell types

A series of CDK inhibitors play key roles in cell cycle, particularly in the G1 phase (29). Therefore, we assessed the mRNA levels of the CDK inhibitors p16, p19, p21, and p27 at 12, 16, and 24 h after plating control and AS160-depleted 3T3-L1 fibroblasts. Whereas p21 expression was markedly upregulated in AS160-depleted cells at 12 and 16 h, p16, p19, and p27 were unchanged (Fig. 3A), and this upregulation of p21 induced by AS160 depletion was further supported by the determination of the protein levels in 3T3-L1 fibroblasts (Fig. 3B). We suspected that this AS160-depletion-induced upregulation of p21 is likely to be of general physiological significance, and thus measured p21 protein levels in MCF7, HeLa, Huh7, and HEK-293 cells. Our results showed that in these cells, 2 siRNAs targeting distinct sequences efficiently depleted AS160 and led to upregulated p21 protein expression at both 48 and 72 h of silencing (Fig. 3C).

Activation of G1-phase CDKs is also known to lead to the phosphorylation of retinoblastoma protein (Rb), a critical downstream effector in the p21-CDK4/6 axis that regulates the expression of a host of target genes through interactions with E2F and other transcription factor complexes.[20-23] Therefore, we evaluated phosphorylated-Rb as a downstream readout of changes in p21: In a line with the p21 upregulation induced by AS160 knockdown, phosphorylated-Rb levels were suppressed in 3T3-L1 fibroblasts following AS160 depletion (Fig. 3D).

AS160 overexpression or p21 silencing in AS160-depeleted cells rescues AS160-depletion-induced blunted cell proliferation and cell cycle

Because AS160 depletion resulted in an upregulation of p21, we speculated that this negative correlation between AS160 and p21 could be revealed by performing double-knockdowns of AS160 and p21 or by overexpressing AS160. However, transfecting the siRNAs into 3T3-L1 fibroblasts efficiently was challenging, and thus we introduced p21 and/or AS160 siRNAs into MCF7 cells. In agreement with the data presented in the preceding subsection, both of the AS160 siRNAs efficiently knocked down the AS160 protein expression and induced a similar amount of p21 increase in MCF7 cells (Figs 4A, B), which precisely matched the increased percentage (58.83%) of AS160-depleted cells arrested in the G1 phase as compared to the fraction (44.18%) of scramble cells arrested in G1 (Fig. 4C, D).

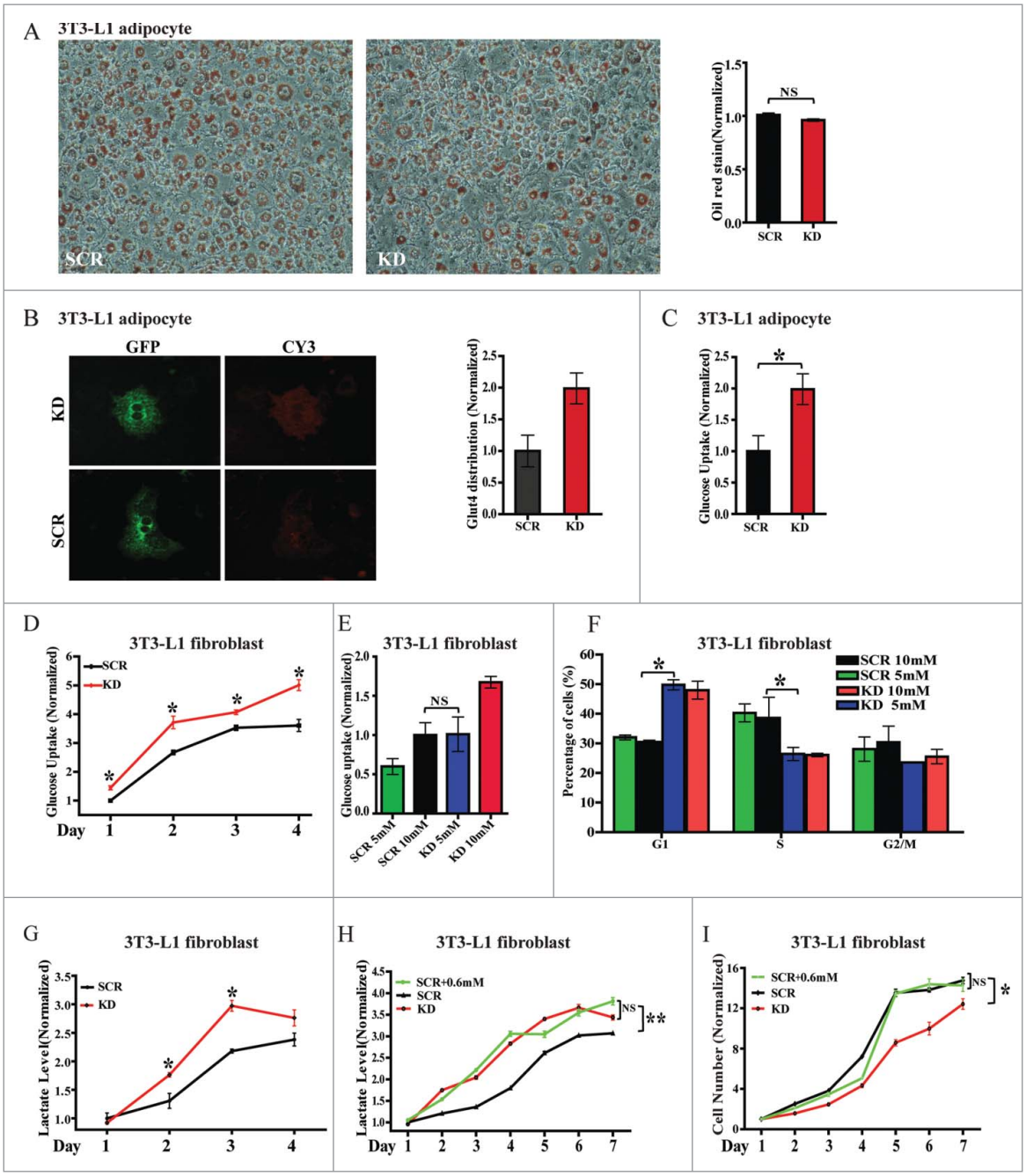

Figure 2. Altering glucose or lactate does not rescue AS160-depletion-induced blunted cell proliferation or cell cycle arrest in G1 in 3T3-L1 fibroblasts. (A) Representative images of oil-red-stained 3T3-L1 adipocytes infected with scrambled (SCR) or AS160-specific shRNA (KD). Quantified Results represent normalized mean±s .e.m. of OD values of oil-red staining (right, $n = 3$ represents 3 replicated experiments, same below); here and below, NS, not significant. (B) Representative GFP and Cy3 images of 3T3-L1 SCR and KD adipocytes electroporated with the HA-GLUT4-GFP construct and immunostained with Cy3-conjugated HA antibodies in the basal state. Quantified data represent normalized Cy3/GFP fluorescence ratio (right, $n = 3$). (C) Glucose uptake into 3T3-L1 adipocytes from (B), determined by measuring glucose in the supernatant and the cell numbers. Data represent normalized mean ± s.e.m. ($n = 3$); $^{*}p < 0.05$, 2-tailed t test, same below. (D) Glucose uptake into 3T3-L1 SCR and KD fibroblasts in a 4-d period of cell proliferation. Data represent normalized mean ± s.e.m. ($n = 3$); here and below, $^{*}p < 0.05$ compare to SCR, t test. (E) Glucose uptake into 3T3-L1 SCR and KD fibroblasts exposed to the indicated glucose concentration in the culture medium. The amounts of glucose taken up into the fibroblasts were equal when 10 mM glucose was included in the medium used for SCR cells and 5 mM glucose was added in the medium for KD cells. The result represent mean ± s.e.m. ($n = 4$). (F) Cell cycle analysis of 3T3-L1 fibroblasts from (E). Data shown are mean ± s.e.m. ($n = 4$); $^{*}p < 0.05$, t test. G, Lactate levels in the supernatants of 3T3-L1 SCR and KD fibroblasts in a 4-d period of cell proliferation ($n = 3$). H, Lactate levels in the supernatants of 3T3-L1 SCR and KD fibroblasts in a 7-d period of cell proliferation. The lactate levels were equal in the supernatants of KD and SCR cells when the SCR cell-culture medium was supplemented an extra 0.6 mM lactate ($n = 3$); $^{**}p < 0.01$, t test. I, Proliferation of 3T3-L1 fibroblast from (H) was quantified through cell counting and normalized relative to the initial cell numbers. Results represent normalized mean ± s.e.m. ($n = 3$).

Next, we found that 2 siRNAs against p21, p21-KD1 and p21-KD2, induced the G1 arrest of 33.93% and 40.36% of the cells, respectively (Fig. 4C, D), which was correlated with the levels to which p21 protein expression was silenced by these siRNAs (p21-KD1 was more effective than p21-KD2; Fig. 4A, B). Interestingly, p21 silencing did not affect the expression of AS160 (Fig. 4A, B).

We also introduced p21 siRNAs into AS160-silenced cells. As per our expectation, this led to a marked rescue of the cells in G1: the fraction was lowered to 47.72% (compared to

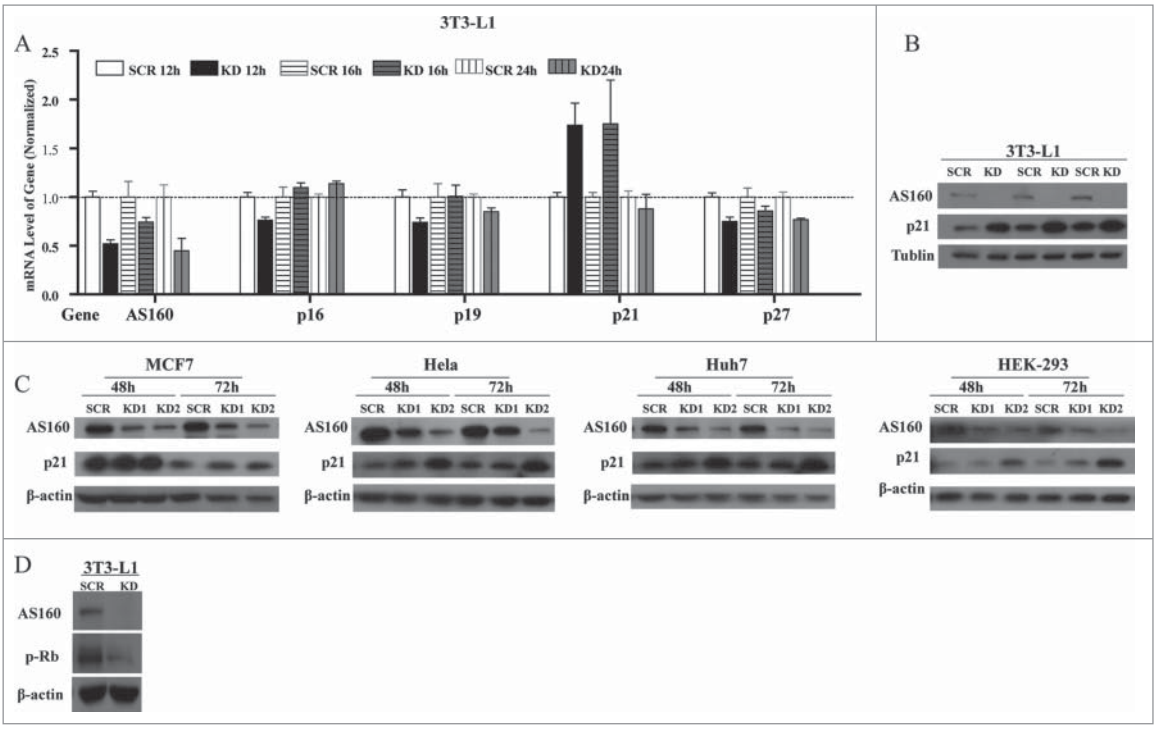

Figure 3. AS160 knockdown upregulates the CDK inhibitor p21 in multiple cell types. (A) Screening of mRNA levels of AS160, p16, p19, p21, and p27 in 3T3-L1 fibroblasts infected with scrambled (SCR) or AS160-specific (KD) shRNAs, at indicated times post-plating. Data shown are normalized mean ± s.e.m. ($n = 3$ represents 3 replicated experiments, same blow). (B) Levels of the indicated proteins in 3T3-L1 SCR and KD fibroblasts, determined with triplicated sample loading. Tubulin severed as the loading control. (C) Western blots of MCF7, HeLa, Huh7, and HEK-293 cells transfected with 2 AS160 siRNAs (KD1 and KD2) or a scrambled siRNA (SCR), at 48 and 72 h post-transfection. (D) Protein levels of phosphorylated-Rb and AS160 in 3T3-L1 SCR and KD fibroblasts.

58.83% in the case of AS160-silenced cells or 44.18% for scramble cells) (Fig. 4A, B, C, D).

To examine in detail the mechanism of action of AS160 in the regulation of cell cycle and proliferation, we next overexpressed wild-type (WT) AS160 in the AS160-silenced cells; our results showed that this again led to a marked rescue of cells in the G1 phase: the fraction was lowered to 48.77% (compared to 58.83% for AS160-silenced cells), which fit well with p21 downregulation through the overexpression of WT-AS160 in the AS160-silenced cells (Fig. 4A, B). Moreover, this effect was not limited to MCF7 cells: a similar result was obtained with HEK-293 cells (Fig. S2).

In another set of experiments, we plated the transfected cells and measured cell proliferation. In agreement with the cell cycle data, these results showed that p21 silencing in AS160-KD1 cells (Fig. 4E) or -KD2 cells (Fig. 4F) potently rescued the inhibited cell proliferation caused by AS160 depletion in MCF7 cells. Furthermore, we observed that the p21-silenced cells tended to show an increased growth rate.

Collectively, the results of this study demonstrated that 1) AS160 regulates cell proliferation and cell cycle in multiple cell types; 2) AS160-regulated cell proliferation is not related to glucose uptake and metabolism; and 3) AS160 negatively modulates the expression of the CDK inhibitor p21. These findings reveal a detailed and clear-cut function and a previously unrecognized mechanism of action of AS160 in the regulation of glucose-independent cell proliferation, which involves AS160 modulation of p21-dependent control of the cell cycle.

Discussion

In this study, we comprehensively investigated the details of AS160-regulated cell proliferation in multiple cell types. We found that AS160 silencing led to blunted cell proliferation in 3T3-L1 fibroblasts and other cells, including MCF7 and Huh7 cells. Therefore, this regulation might not limited to β-cells,[6] breast cancer,[19] the multiple types of cells in this study and could be of general physiological significance.

Previously, AS160 knockdown was shown to result in a partial redistribution of GLUT4 from intracellular compartments to the plasma membrane, a concomitant increase in basal glucose uptake, and a 3-fold increase in basal GLUT4 exocytosis.[24] In agreement with this report, in our study, cultured AS160-depleted 3T3-L1 cells differentiated into adipocytes normally, and under basal conditions, both GLUT4 distribution to the plasma membrane and glucose uptake in these cells were increased; this demonstrated that a normal and functional differentiated cell system was obtained using our cultures. Considering the crucial role that AS160 plays in glucose metabolism and energy homeostasis,[15,25,26] we initially suspected that AS160-dependent regulation of cell proliferation might be related to increased glucose uptake and metabolism. Thus, we sought to confirm the effect of glucose on the blunted cell proliferation, and therefore modulated glucose concentrations in the culture medium to ensure equal glucose uptake into scramble and AS160-depleted cells (Fig. 2E). Unexpectedly, we detected no differences in cell cycle characteristics between normal scramble cells and scramble cells exposed to altered glucose levels, or between AS160-depleted cells and AS160-depleted

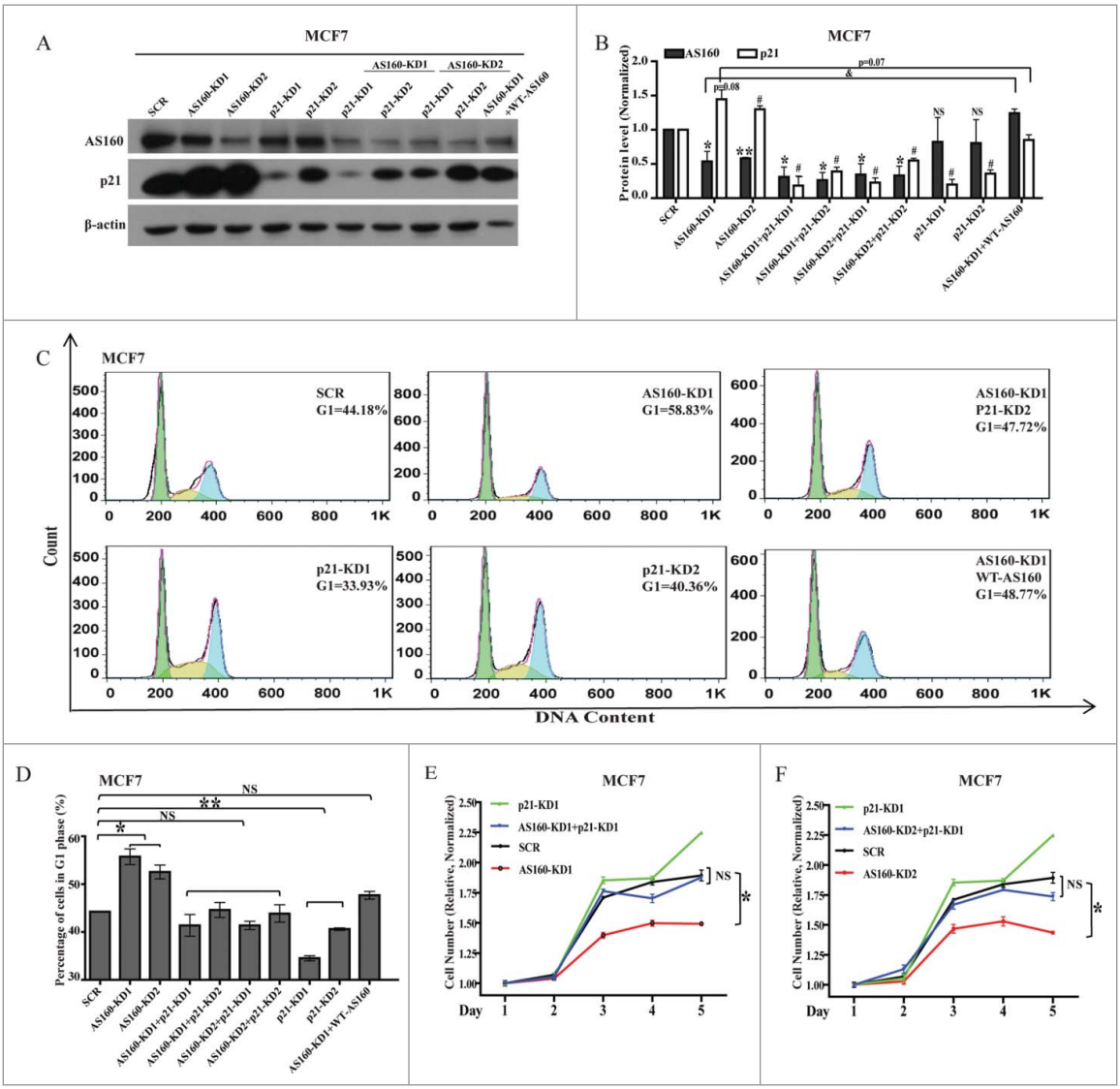

Figure 4. p21 silencing or AS160 overexpression in AS160-silenced cells rescues blunted cell cycle and cell proliferation caused by AS160 knockdown. (A) Levels of indicated proteins in MCF7 cells transfected with 2 AS160 siRNAs (AS160-KD1 and AS160-KD2) and/or p21 siRNAs (p21-KD1 and p21-KD2), scrambled siRNA (SCR), or a wild-type AS160 construct (WT AS160), as indicated. (B) Quantified levels of p21 and AS160 proteins from (A); the data were averaged and normalized relative to the scramble cells, respectively ($n = 3$ represents 3 replicated experiments, same below); here and below, NS, not significant; 2-tailed t test, $^{*}p < 0.05$, $^{**}p < 0.01$ compared to AS160 level of SCR; $\#p < 0.05$ compared to p21 level of SCR; and $p < 0.05$. (C) Cell cycle analysis of MCF7 cells from (A and B). Results represent mean ± s.e.m. ($n = 3$). (D) Quantification of the percentage of cells in G1 phase from (C); $n = 3$, here and below, $^{*}p < 0.05$ and $^{**}p < 0.01$. (E) Proliferation of SCR and KD (AS160-KD1) MCF7 cells from (A–D) was measured using the MTS assay and normalized relative to the initial OD values. Data shown are mean ± s.e.m. ($n = 3$). (F) Proliferation of SCR and KD (AS160-KD2) MCF7 cells from (A–D) was measured using the MTS assay and normalized relative to the initial OD values. Data shown are mean ± s.e.m. ($n = 3$).

cells exposed to altered glucose levels (Fig. 2F). Similarly, altering the lactate level in the culture medium also did not cause any change in cell proliferation (Fig. 2I). Therefore, we propose that the AS160-depletion-induced inhibition of cell proliferation is not related to glucose metabolism.

CDK inhibitors are essential for controlling cell cycle and cell proliferation.[22] The CDK inhibitor p21 is a key regulator of the G1-phase cell cycle checkpoint: p21 functions by inducing cell cycle arrest through CDK inhibition and/or impairment of DNA replication by interacting with proliferating-cell nuclear antigen, a molecular platform for several factors involved in DNA metabolism.[21,23,27] Accurate transition from the G1 phase to S phase of the cell cycle is crucial for the control of eukaryotic cell proliferation, and its misregulation promotes oncogenesis. During the G1 phase, CDK activity promotes DNA replication and initiates G1-to-S transition. Our screening of CDK inhibitors revealed for the first time that p21 was upregulated in multiple AS160-silenced cells, including 3T3-L1 fibroblasts and HeLa, Huh7, and HEK-293 cells (Fig. 3), which demonstrated that AS160-modulated p21 upregulation is of broad physiological significance.

In other assays, we found that overexpression of WT AS160 inhibited p21 expression and rescued the blunted cell cycle and cell proliferation observed following AS160 silencing, but that p21 knockdown did not affect AS160 expression; this finding indicates that AS160 might regulate p21 as an upstream factor. We also attempted to determine whether AS160 regulates the transcriptional or translational process by measuring the half-life of p21 by using the cycloheximide (CHX) chase assay; our data revealed that AS160 depletion

did not affect the half-life of p21. Considering that the p21 mRNA was upregulated following AS160 silencing (Fig. 3A), we collectively propose the radical hypothesis that AS160 functions in the transcriptional process (Fig. S3). The detailed modulation mechanism involved here warrants elucidation in the near future.

In summary, we have shown that AS160 functions in cell proliferation by regulating the expression of the CDK inhibitor p21 and eventually modulating the cell cycle. Our findings reveal a previously unrecognized mechanism of AS160 regulation of cell proliferation that is of general physiological significance.

Materials and methods

Cell culture, differentiation, constructs, viral infections, retroviral shRNA silencing, and electroporation

We tested 3T3-L1 fibroblasts (ATCC, CL-173) for mycoplasma contamination and cultured in DMEM (Hyclone, SH30022.01B) supplemented with 25 mM glucose (Sigma, G8769), 10% calf serum (Bilological Industries, 1421032), and 1% penicillin/streptomycin (Bilological Industries, 1531326) at 37°C and 10% CO_2. To induce the differentiation of 3T3-L1 cells, confluent cells were exposed to an adipogenic mixture for 3 d: 10% FBS (Bilological Industries, 1447832), 1 μM dexamethasone (Adamas, 60231A), 0.5 mM 3-Isobutyl-1-methylxanthine (Sigma, I5879), 1 μM rosiglitazone (Sigma, R2408) and 1 μg/mL insulin (Roche, 11376497001).[28]

HEK-293, MCF7, HeLa, Huh7, and Eco cells were tested for mycoplasma contamination and maintained in DMEM supplemented with 10% FBS and 1% penicillin/streptomycin at 37°C and 10% CO_2.

For stable knockdown of AS160 in 3T3-L1 fibroblasts, oligonucleotides for pSIREN-RetroQ retroviral vectors (Clonetech, PT3739-1) were designed with *Bam*HI- and *Eco*RI-compatible extensions and annealed and cloned into the vectors, and the constructed vectors were sequenced to ensure accuracy. The targets for mouse AS160 and the scrambled oligos were 5′-GACTTAACTCATCCAACGA-3′ and 5′-GCGAAAGATGATAAGCTAA-3′, respectively. Reconstructed retroviral vectors were transfected into Eco packaging cells, and supernatants were collected at 48 h post-transfection, passed through a 0.45-μm nitrocellulose filter, and applied on 3T3-L1 cells together with 5 μg/m polybrene (Sigma, AL-118). The cells were re-infected the next day and selected with 10 μg/mL puromycin (Invitrogen, A1113803) for 5 d.

For transient knockdown of AS160 in other cell lines, 1×10^5 cells were plated in 6-well plates and transfected with 2 siRNAs targeting distinct human AS160 sequences, 5′-GAGCAAGCCTTTGAAATGC-3′ and 5′-GCACAAAGAGAAAGCUGAA-3′, or transfected with the scrambled sequence 5′-TTCTCCGAACGTGTCACGT-3′ (Genepharma, China); HEK-293, MCF7, HeLa, and Huh7 cells were transfected with the siRNAs by using Lipofectamine 3000 (Invitrogen, 1718526).

HA-GLUT4-GFP (a gift from Samuel Cushman, NIH) was transfected into differentiated 3T3-L1 adipocytes by means of electroporation (Eppendorf, Germany). WT AS160 was purchased from Addgene, USA.

Antibody and reagents

The antibodies used in this study were against AS160 (Millipore, 07-741), phosphorylated-Rb (CST, 9308), β-tubulin (CST, 2128), β-actin (Santa Cruz, sc-81178), HA.11 (Covance, MMS-101P), Cy3 Goat Anti-Mouse IgG (Jacksonimmuno, 115-165-003) and p21 (BD Biosciences, ab109199).

PtdIns, RNase, and oil red were obtained from Sigma-Aldrich (25535-16-4, 9001-99-4, O0625 respectively). Cell viability was measured using the Cell Titer GloH Luminescent Cell Viability Assay (Promega, G358A). Lipofectamine 3000 transfection reagent and SYBR® Green Master Mix were purchased from Invitrogen, USA (150603).

Glucose and lactate measurements

Supernatants of cultured 3T3-L1 fibroblasts were collected at various times (indicated in figures) during the culture period; cell proliferation was evaluated at the time points and the lactate and glucose were measured using the respective kits (NanJingJiancheng, China). Subsequently, the quantified values were standardized using the measured cell numbers (see "Cell-proliferation assay").

Cell cycle and apoptosis analysis

Scramble and AS160-depleted 3T3-L1 fibroblasts were cultured for 24 h before cell cycle analysis, whereas MCF7 cells were cultured for 30 h after siRNA transfection. The cells were fixed with 70% (v/v) cold ethanol overnight, washed once with phosphate-buffered saline (PBS), and resuspended in 500 μL of PBS containing 100 μg/mL RNase for 30 min at 37°C, and then incubated (for 15 min) with the nuclear stain PI at a final concentration of 40 μg/mL. We analyzed 1×10^4 cells/sample by using a BD AccuriC6 flow cytometer (BD Biosciences, USA).

Apoptosis of 3T3-L1 fibroblasts was assessed by using Annexin V-FITC/PtdIns kits (Invitrogen, USA) according to the manufacturer's instructions. Stained cells were analyzed by means of flow cytometry performed using the BD AccuriC6 flow cytometer. Cell cycle and apoptosis levels were further analyzed using FlowJo software.

Cell-proliferation assay

Cells were seeded in 96-well plates at 0.5×10^4 cells/well and cultured for different number of days (indicated in figures). To count 3T3-L1 fibroblasts, nuclei were stained with 4′,6-diamidino-2-phenylindole (DAPI) and then the cells were imaged (Nikon Ti-E, Japan) and their numbers were determined using MetaMorph software (Molecular Devices, USA). For MCF7 and Huh7 cells, 3-(4,5-dimethylthiazol-2-yl)-5-(3-carboxymethoxyphenyl)-2-(4-sulfophenyl)-2H-tetrazolium (Promega, G3582) was diluted 1:4 with fresh culture medium and this mixture was added to cells in 96-well plates; the cells were incubated with the mixture for 4 h, and then the color intensity, which reflects cell viability, was measured at 492 nm. The quantifications of cell proliferation were normalized relative to the initial nucleus numbers (3T3-L1 fibroblasts) or optical density (OD) values (MCF7 and Huh7 cells).

Western blotting analysis

Cells were rinsed twice with ice-cold PBS and then lysed in appropriate RIPA extraction buffer (Beyotime, P0013C) on ice for 30 min by pipetting several times every 5 min. Protein samples were separated using sodium dodecyl sulfate–polyacrylamide gel electrophoresis (SDS—PAGE) and transferred to polyvinylidene fluoride (PVDF) membranes (Millipore, IPVH00010). Membranes were blocked in 5% skim milk in Tris-Buffered Saline and Tween 20 (TBST) for 1 h and then incubated with primary antibodies in TBST containing 3% skim milk (4°C, overnight). After rinsing 5 times in TBST, membranes were incubated with secondary antibodies for 2 h at room temperature in TBST containing 3% skim milk, rinsed again in TBST, and then developed using Western Lightning Chemiluminescence Reagent (Perkin-Elmer Life Science, USA). Protein bands in western blots were quantified using MetaMorph software.

Quantitative PCR

We used quantitative PCR (qPCR) to examine the mRNA levels of AS160, p16, p19, p21, and p27 in scramble and stable-AS160-knockdown 3T3-L1 fibroblasts. Total RNAs were prepared from cultured cells by using TRIzol A reagents (Invitrogen, 15596026), and 1 μg of total RNA was reverse-transcribed using a cDNA Synthesis Kit (Bio-Rad, K1622). The primers for qPCR were the following:

P21: F-CCTGGTGATGTCCGACCTG, R-CCATGAGCGC ATCGCAATC;
P19: F-CTGAACCGCTTTGGCAAGAC, R-GCCCTCTCTTATCGCCAGAT;
P16: F-GCTCAACTACGGTGCAGATTC, R-GCACGATGTCTTGATGTCCC;
P27: F-TAATTGGGGCTCCGGCTAACT, R-TGCAGGTCGCTTCCTTATTCC;
AS160: F-GCATTCAGGATGAGCCTTTCC, R-CTCCCACGTACCATAGCCG;
β-actin: F-GGCTGTATTCCCCTCCATCG, R-CCAGTTGGTAACAATGCCATGT.

Statistics

Statistical analysis to calculate P-value was carried out using a 2-tailed t test. The level of significance was set to $P<0.05$ or as indicated in Figure Legends.

Disclosure of potential conflicts of interest

No potential conflicts of interest were disclosed.

Acknowledgments

We thank Dr. Samuel Cushman for generously providing the HA-GLUT4-GFP vector.

Funding

This work was supported by the Chinese Academy of Sciences (292013312D11004 to W.X.); and the National Sciences Foundation of China (81270919 to W.X.) and Sciences Foundation of Yunnan Province (39Y33H521261 to W.X.).

Author contributions

P.G. and W.X. designed research; P.G. and Y.L. performed research; F.W. and Y.X. analyzed data; and P.G. and W.X. wrote the paper.

References

[1] Kane S, Sano H, Liu SC, Asara JM, Lane WS, Garner CC, Lienhard GE. A method to identify serine kinase substrates. Akt phosphorylates a novel adipocyte protein with a Rab GTPase-activating protein (GAP) domain. J Biol Chem 2002; 277:22115-8; PMID:11994271; http://dx.doi.org/10.1074/jbc.C200198200
[2] Jung HJ, Kwon T-H. Membrane Trafficking of Collecting Duct Water Channel Protein AQP2 Regulated by Akt/AS160. Electrolyte Blood Press 2010; 8:59-65; http://dx.doi.org/10.5049/EBP.2010.8.2.59
[3] Kim HY, Choi HJ, Lim JS, Park EJ, Jung HJ, Lee YJ, Kim SY, Kwon TH. Emerging role of Akt substrate protein AS160 in the regulation of AQP2 translocation. Am J Physiol Renal Physiol 2011; 301:F151-61; PMID:21511697; http://dx.doi.org/10.1152/ajprenal.00519.2010
[4] Alves DS, Thulin G, Loffing J, Kashgarian M, Caplan MJ. Akt Substrate of 160 kD Regulates Na+,K+-ATPase Trafficking in Response to Energy Depletion and Renal Ischemia. J Am Soc Nephrol 2015; 26:2765-76; PMID:25788531; http://dx.doi.org/10.1681/ASN.2013101040
[5] Liang X, Butterworth MB, Peters KW, Frizzell RA. AS160 modulates aldosterone-stimulated epithelial sodium channel forward trafficking. Mol Biol Cell 2010; 21:2024-33; PMID:20410134; http://dx.doi.org/10.1091/mbc.E10-01-0042
[6] Bouzakri K, Ribaux P, Tomas A, Parnaud G, Rickenbach K, Halban PA. Rab GTPase-activating protein AS160 is a major downstream effector of protein kinase B/Akt signaling in pancreatic beta-cells. Diabetes 2008; 57:1195-204; PMID:18276765; http://dx.doi.org/10.2337/db07-1469
[7] Watson RT, Pessin JE. Bridging the GAP between insulin signaling and GLUT4 translocation. Trends Biochem Sci 2006; 31:215-22; PMID:16540333; http://dx.doi.org/10.1016/j.tibs.2006.02.007
[8] Bai L, Wang Y, Fan JM, Chen Y, Ji W, Qu AL, Xu PY, James DE, Xu T. Dissecting multiple steps of GLUT4 trafficking and identifying the sites of insulin action. Cell Metab 2007; 5:47-57; PMID:17189206; http://dx.doi.org/10.1016/j.cmet.2006.11.013
[9] Sano H, Eguez L, Teruel MN, Fukuda M, Chuang TD, Chavez JA, Lienhard GE, McGrau TE. Rab10, a target of the AS160 rab GAP, is required for insulin-stimulated translocation of GLUT4 to the adipocyte plasma membrane. Cell Metab 2007; 5:293-303; PMID:17403373; http://dx.doi.org/10.1016/j.cmet.2007.03.001
[10] Sun Y, Bilan PJ, Liu Z, Klip A. Rab8A and Rab13 are activated by insulin and regulate GLUT4 translocation in muscle cells. Proc Natl Acad Sci U S A 2010; 107:19909-14; PMID:21041651; http://dx.doi.org/10.1073/pnas.1009523107
[11] Wang HY, Ducommun S, Quan C, Xie B, Li M, Wasserman DH, Sakamoto K, Mackintosh C, Chen S. AS160 deficiency causes whole-body insulin resistance via composite effects in multiple tissues. Biochem J 2013; 449:479-89; PMID:23078342; http://dx.doi.org/10.1042/BJ20120702
[12] Karlsson HKR, Zierath JR, Kane S, Krook A, Lienhard GE, Wallberg-Henriksson H. Insulin-stimulated phosphorylation of the Akt substrate AS160 is impaired in skeletal muscle of type 2 diabetic subjects. Diabetes 2005; 54:1692-7; PMID:15919790; http://dx.doi.org/10.2337/diabetes.54.6.1692
[13] Ducommun S, Wang HY, Sakamoto K, MacKintosh C, Chen S. Thr (649)Ala-AS160 knock-in mutation does not impair contraction/AICAR-induced glucose transport in mouse muscle. Am J Physiol-Endocrinol Metab 2012; 302:E1036-E43; PMID:22318952; http://dx.doi.org/10.1152/ajpendo.00379.2011
[14] Dash S, Sano H, Rochford JJ, Semple RK, Yeo G, Hyden CS, Soos MA, Clark J, Rodin A, Langenberg C, et al. A truncation mutation in TBC1D4 in a family with acanthosis nigricans and postprandial

hyperinsulinemia. Proc Natl Acad Sci U S A 2009; 106:9350-5; PMID:19470471; http://dx.doi.org/10.1073/pnas.0900909106

[15] Hargett SR, Walker NN, Keller SR. Rab GAPs AS160 and Tbc1d1 play nonredundant roles in the regulation of glucose and energy homeostasis in mice. Am J Physiol Endocrinol Metab 2016; 310:E276-88; PMID:26625902; http://dx.doi.org/10.1152/ajpendo.00342.2015

[16] Quan C, Xie B, Wang HY, Chen S. PKB-Mediated Thr649 Phosphorylation of AS160/TBC1D4 Regulates the R-Wave Amplitude in the Heart. PLoS One 2015; 10:e0124491; PMID:25923736; http://dx.doi.org/10.1371/journal.pone.0124491

[17] Wu LZ, Xu DJ, Zhou LK, Xie BX, Yu L, Yang HY, Huang L, Ye J, Deng HT, Yuan YA, et al. Rab8a-AS160-MSS4 Regulatory Circuit Controls Lipid Droplet Fusion and Growth. Dev Cell 2014; 30:378-93; PMID:25158853; http://dx.doi.org/10.1016/j.devcel.2014.07.005

[18] Rutti S, Arous C, Nica AC, Kanzaki M, Halban PA, Bouzakri K. Expression, phosphorylation and function of the Rab-GTPase activating protein TBC1D1 in pancreatic beta-cells. FEBS Lett 2014; 588:15-20; PMID:24239544; http://dx.doi.org/10.1016/j.febslet.2013.10.050

[19] Jiang XH, Sun JW, Xu M, Jiang XF, Liu CF, Lu YA. Frequent hyperphosphorylation of AS160 in breast cancer. Cancer Biol Therapy 2010; 10:362-7; PMID:20574165; http://dx.doi.org/10.4161/cbt.10.4.12426

[20] Dowling RJ, Topisirovic I, Alain T, Bidinosti M, Fonseca BD, Petroulakis E, Wang X, Larsson O, Selvaraj A, Liu Y, et al. mTORC1-mediated cell proliferation, but not cell growth, controlled by the 4E-BPs. Science 2010; 328:1172-6; PMID:20508131; http://dx.doi.org/10.1126/science.1187532

[21] Abbas T, Dutta A. p21 in cancer: intricate networks and multiple activities. Nat Rev Cancer 2009; 9:400-14; PMID:19440234; http://dx.doi.org/10.1038/nrc2657

[22] Xiong Y, Hannon GJ, Zhang H, Casso D, Kobayashi R, Beach D. P21 Is a Universal Inhibitor of Cyclin Kinases. Nature 1993; 366:701-4; PMID:8259214; http://dx.doi.org/10.1038/366701a0

[23] Prives C, Gottifredi V. The p21 and PCNA partnership: a new twist for an old plot. Cell Cycle 2008; 7:3840-6; PMID:19066467; http://dx.doi.org/10.4161/cc.7.24.7243

[24] Brewer PD, Romenskaia I, Kanow MA, Mastick CC. Loss of AS160 Akt Substrate Causes Glut4 Protein to Accumulate in Compartments That Are Primed for Fusion in Basal Adipocytes. J Biol Chem 2011; 286:26287-97; PMID:21613213; http://dx.doi.org/10.1074/jbc.M111.253880

[25] Chen SA, Wasserman DH, MacKintosh C, Sakamoto K. Mice with AS160/TBC1D4-Thr649Ala Knockin Mutation Are Glucose Intolerant with Reduced Insulin Sensitivity and Altered GLUT4 Trafficking. Cell Metab 2011; 13:68-79; PMID:21195350; http://dx.doi.org/10.1016/j.cmet.2010.12.005

[26] Funai K, Schweitzer GG, Castorena CM, Kanzaki M, Cartee GD. In vivo exercise followed by in vitro contraction additively elevates subsequent insulin-stimulated glucose transport by rat skeletal muscle. Am J Physiol-Endocrinol Metab 2010; 298:E999-E1010; PMID:20179245; http://dx.doi.org/10.1152/ajpendo.00758.2009

[27] Dotto GP. p21(WAF1/Cip1): more than a break to the cell cycle? Biochimica Et Biophysica Acta-Reviews on Cancer 2000; 1471:M43-M56; http://dx.doi.org/10.1016/S0304-419X(00)00019-6

[28] Xiong W, Jordens I, Gonzalez E, McGraw TE. GLUT4 is sorted to vesicles whose accumulation beneath and insertion into the plasma membrane are differentially regulated by insulin and selectively affected by insulin resistance. Mol Biol Cell 2010; 21:1375-86; PMID:20181829; http://dx.doi.org/10.1091/mbc.E09-08-0751